Solar Energy 202 (2020) 409–419

Contents lists available at ScienceDirect

Solar Energy

journal homepage: www.elsevier.com/locate/solener

Robust Model Predictive Control (MPC) for large-scale PV plant based on paralleled three-phase inverters

S. Bella[a,b,*], A. Houari[b], A. Djerioui[a,b], A. Chouder[a], M. Machmoum[b], M.-F. Benkhoris[b], K. Ghedamsi[c]

[a] LGE Laboratory, University of M'sila, Algeria
[b] IREENA Laboratory, Nantes University, Saint-Nazaire 44600, France
[c] LMER Laboratory, University of Bejaia, Algeria

ARTICLE INFO

Keywords:
Grid-connected inverter
Parallel operation
Circulating current
PV power plant
Model predictive control
Hardware-in-the-loop

ABSTRACT

In this contribution a robust Model Predictive Control (MPC) is proposed to enhance the power quality of a large-scale PV plant connected to the grid through Paralleled Voltage Source Inverters (PVSIs) with common AC and DC buses. Paralleling inverters allow handling high-power export and offer advantages in terms of redundancy which ensure the system reliability. However, due to the physical differences and parameter disparities between the inverters, zero sequence circulating currents will flow through it, which will disturb the performance of the system. Hence, the control goal is to regulate the currents injected into the grid, suppress the zero-sequence circulating current (ZSCC). Consequently, this study proposes an MPC algorithm that is based on optimization approach which allows minimizing circulating currents. In order to show its effectiveness and performance of the proposed control, a comparison with linear PI controller is included. In addition, design control and tuning procedure are detailed. Simulation results show the performance of the proposed controller in ensuring power quality, and suppressing circulating currents. To verify the real-time feasibility of the proposed control scheme, Hardware-In-the-Loop (HIL) setup is carried out with means of Opal-RT and dSPACE rapid prototyping systems.

1. Introduction

Large-scale photovoltaic plants (LSPPs) are being a viable solution to handle the growth of green energy sources integration as they provide an interesting mid-term return of investment ("IEA PVPS report, 2018"; Tang, 2017; Tobar and Karina, 2018). This is essentially due to the decrease of the manufacturing cost of PV modules as reported by the International Energy Agency (IEA). Actually, PV modules prices have fallen by nearly 70% and are expected to continue to decline for future large-scale PV systems ("IEA report," 2018). LSPPs are capable to generate power in range of megawatts such that installed in Australia in 2018 which is the largest one in the country with the capacity of 220 MW ("M. Maisch," 2018). As the produced energy by these PV plants is intended to be injected in the main grid, some challenges will arise due to the necessity of feeding it in a smooth and efficient way. Besides, due to the power rating limitations of the existing power inverters and economic issues, it is difficult to deliver this power to the main grid with a single central inverter. For such systems, in which efficiency and power quality should comply with international standards (Ouai et al., 2018; Wu et al., 2017; Xu et al., 2019), paralleling inverters seem to be a promising solution. This topology, based on paralleled three-phase inverters, allows energy availability of the system even in case of partial failure. Furthermore, they ensure the improvement of efficiency since components are less stressed (Bella et al., 2018a, 2018b; Zhang et al., 2018). However, when parallel inverters are connected in the same DC and AC buses, undesired current known as zero-sequence circulating current (ZSCC) appears through inverters. Basically, the main reason of emerging such a problem is the disparities between the parameters of inverters, tolerance of hardware devices, unequal filters, dead-time, and asynchronous switching frequencies (Wang et al., 2018; Wei et al., 2017). The existence of this current might lead to the distortion of the line-currents of each inverter, increases power losses, and decreases the efficiency of the whole system.

Various methods have been reported to solve this issue. For instance, some industrials suggest to install multi-port isolating transformers in the AC side of the central inverter (Jun-Keun Ji ; Seung-Ki Sul, 1999), such that PVS800 solar inverter ("ABB, PVS800"), and SGI 500/750XTM solar inverter ("SGI 500/750XTM"). This method can definitely stop the ZSCC from flowing through inverters. However, it is expensive, bulky, and transformers suffer from losses; which make this

* Corresponding author.
E-mail addresses: saad.bella@univ-msila.dz, saad.bella@univ-nantes.fr (S. Bella).

https://doi.org/10.1016/j.solener.2020.03.091
Received 14 May 2019; Received in revised form 7 February 2020; Accepted 23 March 2020

Nomenclature

PVSIs	Parallel voltage source inverters
ZSCC	Zero-sequence circulating current
LSPPs	Large-scale photovoltaic plant
MPPT	Maximum power point tracking
P&O	Perturb and observe algorithm
CCs	Circulating currents
CMV	Common-mode voltage
THD	Total harmonic distortion
$v_{abc(i)}$	are the output voltages of the inverter(i)
e_{abc}	represent the grid voltages
$i_{abc(i)}$	the phase currents of the inverter(i)
θ	grid angle
ω	grid frequency
P_{gref}	the reference of active power injected into the grid
Q_{gref}	the reference of reactive power injected into the grid
P_{loss}	the power dissipation
P_{PV}	maximum power available power of the PV plant
n	number of the modules composed in parallel
MPC	Model predictive control
FCS-MPC	Finite control set predictive control
T_s	sampling time
N_P	prediction horizon
N_C	control horizon
K_{mpc}	feedback control gain using MPC
$x(k+T)$	Predicted state variable vector at sample time T, given current state
$\Delta u(k)$	Incremental control at sample
ΔU	Parameter vector for the control sequence in discrete time MPC
ξ	Damping coefficient in PI controller design

solution usually limited to two paralleled inverters. In (Xueguang et al., 2014; Ye et al., 2002), a PI controller has been introduced to modify the distribution of zero vectors at each switching period of space vector modulation (PWM). However, the PI controller is sensitive to the change of parameters which leads to poor performance. Other research has investigated that the emerging of circulating currents (CCs) is due to the asynchronized PWM and the interaction between inverters. Therefore, in order to eliminate (CCs) two parallel two-level inverters are controlled as one three-level inverter (Ogasawara et al., 1992; Quan and Li, 2017). This method is capable to eliminate ZSCC. But, if more than two inverters are connected in parallel the control becomes too complicated. Further, it does bring unwanted currents called cross currents. To deal with this last issue, a control method was proposed for minimizing cross currents by introducing a control variable to adjust the duration time of the switching vectors (Zorig et al., 2017). However, it is still complicated, and difficult to implement in more than two parallel inverters.

Several studies have shown that the ZSCC is closely related to the difference of common mode voltage (CMV) between VSIs. Therefore, the suppression of circulating current is achieved by injecting the same CMV in each inverter of the parallel system or by synchronizing their PWM carriers (Chen, 2009; Jiang et al., 2018; Prasad et al., 2015). However, even they will have the same CMV, ZSCC will still possible circulate if the fundamental component of CMV of inverters are different.

Today, the power electronic application community has begun adopting the concept of MPC from control system theory (Lim et al., 2014). Indeed, predictive control is largely used to control power electronics based applications (Chai et al., 2013; Lim et al., 2014; Yaramasu et al., 2013). This is due to its proprieties that make it suitable for the control of power inverters: simple concept, possibility of including nonlinearities, it considers multivariable approach, and the implementation is easy with the development of processors. Many algorithms are applied in power electronics, amongst them model predictive control (MPC) was proposed for electric drives-based application, where it is applied to control PMSM (Chai et al., 2013). Another variety of MPC called finite set control model predictive (FSC-MPC) is applied to control grid-connected converters (Yaramasu et al., 2013; Xing et al., 2017; Wang, 2009; Kazmierkowski, 2012). For instance, a Lyapunov function based FSC-MPC was proposed to control PV grid-connected inverter (Boukezata et al., 2016; Golzari et al., 2019). However, greater is the number of switches used, greater is the computational burden. Also, the switching frequency is variable which might produce a large distributed current spectrum, causing resonances, audible noise, and poor steady-state behavior.

In this work, a robust predictive algorithm is proposed to handle power quality requirement in large scale PV plant based on paralleled three-phase inverters. The main motivation is related to the promising performance of predictive control to handle complex control issues.

The main purpose is to assess the performance of paralleled inverters in order to remove the undesired circulating current and ensure power quality requirements. The main contribution and the novelty of the present work can be summarized in the following points:

- Parallel inverter structure is used to export power from large-scale PV plant to the main grid which offers high efficiency and availability under existing failure.
- Robust Model Predictive Control MPC is proposed to ensure the proper control of delivered power to meet the requirement of grid integration code. This algorithm is extended in such way to provide an appropriate augmented model which adds an integral action that allows to achieve good tracking, a good steady state, and rejection of unknown disturbances.
- The optimization approach is used to make the control accurate which gives a smooth power and a smaller ripple.
- The z-axis component is included in the cost function for minimizing circulating currents flowing through inverter units
- The proposed MPC control is validated through MatLab Simulink and its real-time feasibility is verified via a Hardware-In-the-Loop (HIL) setup based on Opal-RT and dSPACE rapid prototyping systems.

The proposed MPC is based on an optimization approach which allows minimizing circulating currents with ensuring the standard requirements for the grid. This technique can be generalized to be applied on n-inverters allowing power sharing; which seems to be interesting from industrial point of view given the limitation of central inverter structures. Hence, in order to demonstrate the effectiveness of the proposed control, the performance of the proposed MPC is compared to that of PI controller in terms of power quality, power ripple, perturbation rejection, and good dynamic response.

The rest of this paper is arranged as follows. In Section II, modeling of parallel inverters is analyzed, and, in Section III, designing the proposed MPC controller is presented. Section IV presents simulation results to validate the effectiveness of control scheme. Section V presents the HIL architecture and the obtained results. Finally, section VI is dedicated to the conclusion.

2. System modeling

Fig. 1 depicts a PV plant connected to the main grid through parallel inverters. The structure of the system comprises several three-phase

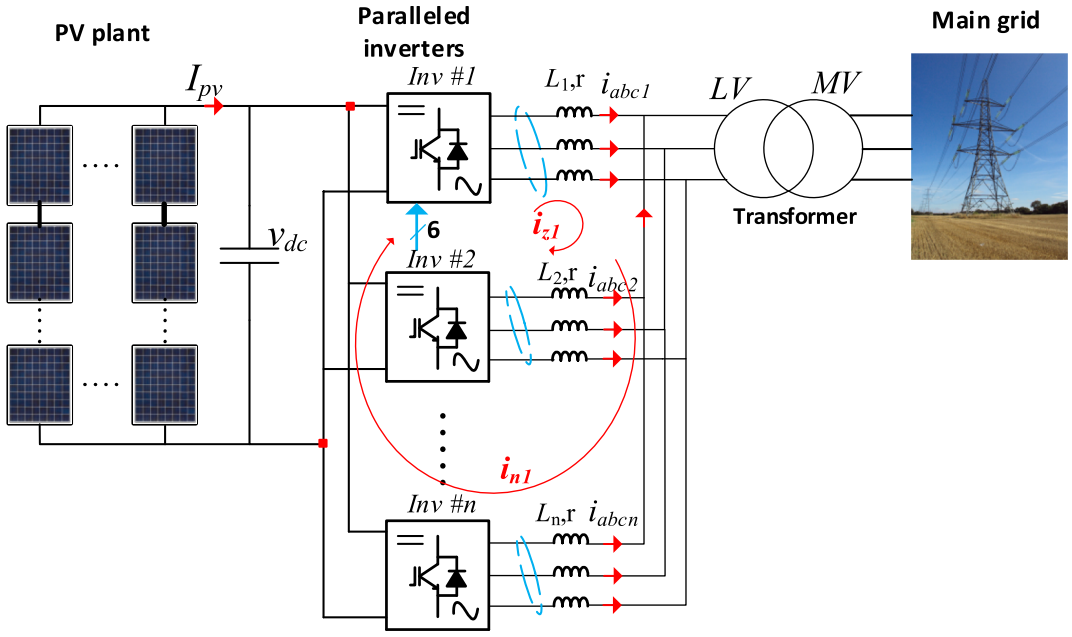

Fig. 1. Structure of the studied system.

voltage source inverters connected in parallel with common DC and AC buses.

In ideal conditions, if the parallel inverters are composed of similar modules and inductances, no circulating current will be generated. However, in practice the existence of a small difference in the inverter parameters can lead to a large circulating current through them.

The equations of the system in the three-phases $a-b-c$ frame can be given as:

$$L_{(i)}\frac{di_{abc(i)}}{dt} = v_{abc(i)} - e_{abc} - ri_{abc(i)} \tag{1}$$

where $v_{abc(i)}$ are the output voltages of the inverter (i; $i = 1, 2, ..n$). e_{abc} and $i_{abc(i)}$ represent the grid voltages and phase currents of the inverter (i) respectively; $L_{(i)}$, r are the inductance and the resistance of the output filters.

In the calculation of predicted currents, a mathematical model in $d-q-z$ is helpful to describe the relationship between the system inputs $v_{dq(i)}$, and the system outputs $i_{dq(i)}$. model of the parallel system in the $d-q-z$ frame can be written as:

$$\begin{cases} L_{(i)}\frac{di_{dq(i)}}{dt} = v_{dq(i)} - e_{dq} - ri_{dq(i)} - jL_{(i)}\omega i_{dq(i)} \\ L_{(i)}\frac{di_{z(i)}}{dt} = [v_{z(i)} - ri_{z(i)}] \end{cases} \tag{2}$$

where $v_{z(i)}$ is the common voltage of the inverter (i);

The sum of ZSCC for n-inverters can be written as

$$\sum_{i=1}^{n} i_{zi} = \sum_{i=1}^{n} (i_{ai} + i_{bi} + i_{ci})/\sqrt{3} = 0 \tag{3}$$

For two inverters, we obtain

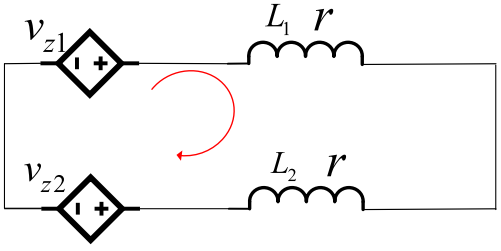

Fig. 2. Dynamic model of ZSCC in two parallel inverters.

$$i_z = i_{z1} = -i_{z2} = (i_a + i_b + i_c)/\sqrt{3} \tag{4}$$

This equation indicates that only one of the two currents is needed to have zero sequence current control.

For three inverters, the expression given by (3) becomes

$$i_{z3} = -(i_{z1} + i_{z2}) \tag{5}$$

This equation indicates that in three parallel inverters only two currents are needed to have zero sequence current control. The dynamic model of the zero-sequence circulating current for two and three parallel inverters can also be deduced from (2). This fact is revealed in Fig. 2 and Fig. 3 respectively.

3. Designing of the proposed MPC controller

This section presents in detail the procedure of designing the proposed MPC control strategy. As illustrated in Fig. 4, the MPC algorithms consist of controlling the line-currents injected to the main grid and minimizing circulating currents through inverters.

The proposed MPC control is designed, on one side to ensure the proper control of the injected currents and on the other side to remove the undesired circulating current in parallel inverters.

The mathematical fundamentals of this control concept is presented

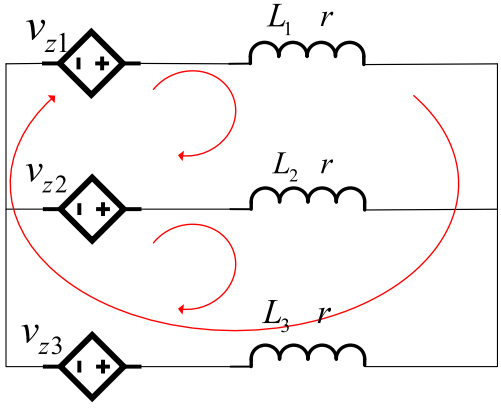

Fig. 3. Dynamic model of ZSCC in three parallel inverters.

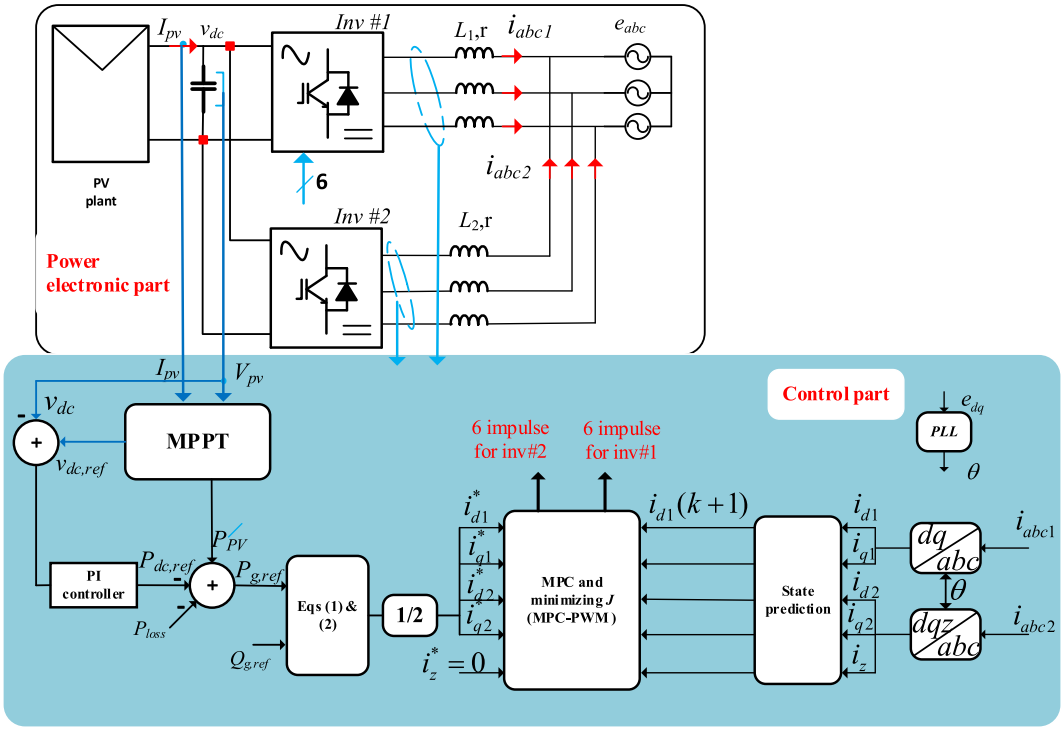

Fig. 4. Block diagram of proposed control scheme for two parallel inverters.

in (Wang, 2009). Actually, the model predictive control is formulated to solve an optimal control problem. Fig. 5 shows the basis of model predictive control. Based on the measured variable, the controller predicts the future dynamic behavior of the system over a prediction horizon N_P. By using a cost function, the objective is to minimize the error between the predicted output and the reference where the objective function is made small as possible. Thus, the control algorithm optimizes over a time period to determine the immediate and best control action that brings the predicted output closer to the desired objective. Once the control is applied, then the controller reinitializes the optimization over the moving horizon to find next control inputs and this keeps marching forward and forward in time.

To build the desired control, it is needed: (i) state prediction, (ii) optimization of the cost function.

(i) State prediction

According to inverter model given above, the dynamic model of the parallel inverters can be written in the following form:

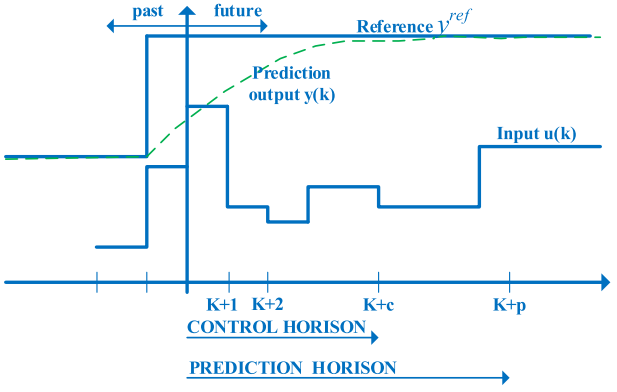

Fig. 5. Principle of the proposed model predictive.

$$\begin{cases} \dot{x}_m(t) = A_m x_m(t) + B_m u(t) + d_m \\ y(t) = C_m x_m(t) \end{cases} \quad (6)$$

where

$$x_m(t) = [i_{d1} i_{q1} i_{d2} i_{q2} i_z]^T$$

$$u(t) = [v_{d1} v_{q1} v_{d2} v_{q2} v_z]^T,$$

$$y(t) = [i_{d1} \;\; i_{q1} \;\; i_{d2} \;\; i_{q2} \;\; i_z]^T$$

and the matrices A_m, B_m, C_m are defined as:

$$A_m = \begin{pmatrix} -r/L_1 & \omega & 0 & 0 & 0 \\ -\omega & -r/L_1 & 0 & 0 & 0 \\ 0 & 0 & -r/L_2 & \omega & 0 \\ 0 & 0 & -\omega & -r/L_2 & 0 \\ 0 & 0 & 0 & 0 & -r/L_2 \end{pmatrix}$$

$$B_m = \begin{pmatrix} 1/L_1 & 0 & 0 & 0 & 0 \\ 0 & 1/L_1 & 0 & 0 & 0 \\ 0 & 0 & 1/L_2 & 0 & 0 \\ 0 & 0 & 0 & 1/L_2 & 0 \\ 0 & 0 & 0 & 0 & 1/L_2 \end{pmatrix}$$

$$C_m = \begin{pmatrix} 1 & 0 & 0 & 0 & 0 \\ 0 & 1 & 0 & 0 & 0 \\ 0 & 0 & 1 & 0 & 0 \\ 0 & 0 & 0 & 1 & 0 \\ 0 & 0 & 0 & 0 & 1 \end{pmatrix}$$

$$d_m = [e_d/L_1 e_q/L_1 e_d/L_1 e_q/L_1 0]^T$$

The state-space model for the parallel grid connected system has to be discretized for the purpose of designing the discrete MPC controller. In this work, Euler approach is used which implies that:

$$A_d \approx I + T_s A_m \& B_d \approx T_s B_m \& C_d = C_m.$$

where $T_s$is the sampling time.

To overcome the uncertainties of unknown parameters, d_m is assumed to be constant in order to be removed when handling the incremental model. By taking the difference between two consecutive samples, the incremental model is given as:

$$\Delta x_m(k+1) = A_d \Delta x_m(k) + B_d \Delta u(k) \tag{7}$$

where

$\Delta x_m(k) = x_m(k) - x_m(k-1)$is the difference of state variable and $\Delta u(k) = u(k) - u(k-1)$ is the difference of control variable also,

$$y(k+1) - y(k) = C_d \Delta x_m(k+1) = C_d A_d \Delta x_m(k) + C_d B_d \Delta u(k) \tag{8}$$

then:

$$y(k+1) = y(k) + C_d A_d \Delta x_m(k) + C_d B_d \Delta u(k) \tag{9}$$

The augmented system can be given as

$$\begin{cases} x(k+1) = Ax(k) + Bu(k) \\ y(k) = Cx(k) \end{cases} \tag{10}$$

where

$$x(k) = \begin{pmatrix} \Delta x_m(k) \\ y(k) \end{pmatrix},$$

$$A = \begin{pmatrix} A_d & 0_{5\times5} \\ C_d A_d & I_{5\times5} \end{pmatrix},$$

$$B = \begin{pmatrix} B_d \\ C_d B_d \end{pmatrix},$$

$$C = (0_{5\times5} \quad I_{5\times5})$$

where $0_{5\times5}$, and $I_{5\times5}$, are the zero and identity matrices respectively, their dimensions are denoted by sub-indices.

This MPC algorithm is used to track the reference signals y^{ref} where for two parallel inverters, the outputs are:

$$y^{ref} = [{i_{d1}}^{ref} {i_{q1}}^{ref} {i_{d2}}^{ref} {i_{q2}}^{ref} {i_z}^{ref}]^T$$

To calculate them, we firstly calculate the reference currents ${i_d}^{ref}$, and ${i_q}^{ref}$ by the following expression

$$\begin{pmatrix} {i_d}^{ref} \\ {i_q}^{ref} \end{pmatrix} = \frac{1}{e_d^2 + e_q^2} \begin{pmatrix} e_d & e_q \\ -e_q & e_d \end{pmatrix} \begin{pmatrix} P_{gref} \\ Q_{gref} \end{pmatrix} \tag{11}$$

Then, dividing them over two in order to make the two inverters sharing the same currents.

The reference currents for each inverter are then calculated as follows:

$${i_{d1}}^{ref} = {i_{d2}}^{ref} = \frac{{i_d}^{ref}}{2} \& {i_{q1}}^{ref} = {i_{q2}}^{ref} = \frac{{i_q}^{ref}}{2} \tag{12}$$

The design of MPC algorithm needs the predicted future outputs for a number of coming steps. The future state vectors predicted for N_P samples from one to N_P instants can be given as

$$x(k+1) = Ax(k) + B\Delta u(k)$$

$$x(k+2) = A^2 x(k) + AB\Delta u(k) + B\Delta u(k+1)$$

$$\vdots$$

$$x(k+N_P) = A^{N_P} x(k) + A^{N_P-1} B^{N_P-1} \Delta u(k) + \cdots + A^{N_P-N_C} B \Delta u(k+N_c-1),$$

where N_c and N_p are named the control and prediction horizon ($N_c \leq N_p$), respectively. Assuming that the incremental control Δu becomes zero after N_c samples. The predicted output vectors for the next N_p instants are written in a compact matrix and vector form, as

$$X = F_x x(k) + \Phi \Delta U \tag{13}$$

where

$$F_x = \begin{bmatrix} A \\ A^2 \\ \vdots \\ A^{N_P} \end{bmatrix}; \Phi = \begin{bmatrix} B & 0 & \cdots & 0 \\ AB & B & \cdots & 0 \\ A^2B & AB & \cdots & 0 \\ \vdots & \vdots & \vdots & \vdots \\ A^{N_P-1}B & A^{N_P-2}B & \cdots & A^{N_P-N_C}B \end{bmatrix}$$

$$\Delta U = [\Delta u(k) \quad \Delta u(k+1) \quad \cdots \quad \Delta u(k+N_C-1)]^T;$$

$$x(k+1) = [x(k+1|k)^T \quad \cdots \quad x(k+N_P|k)^T]^T$$

(ii) Optimization of the cost function

To find the control vector, the following cost function is proposed to be minimized

$$J = X^T \bar{Q} X + \Delta U^T \bar{R} \Delta U \tag{14}$$

where $\bar{Q}$ and $\bar{R}$ are scalar matrices that have identical components. The dimension of the $\bar{Q}$, and $\bar{R}$ matrices are $(5 \times N_p) \times (5 \times N_p)$ and $(5 \times N_c) \times (5 \times N_c)$ for the application of two parallel system. The optimal solution can be given by

$$\frac{\partial J}{\partial \Delta U} = 0$$

Solving this equation gives the optimal control vector as

$$\Delta U = -{\Omega_{mpc}}^{-1} \Psi_{mpc} x(k)$$

where data matrices are defined as

$$\Omega_{mpc} = (\Phi^T \bar{Q} \Phi + \bar{R}) and \Psi_{mpc} = \Phi^T \bar{Q} F_x$$

using receding horizon control, the control components to be applied at the next sampling time (first five rows) is

$$\Delta u(t_i) = -[I\,0 \ldots 0] \widetilde{\Omega_{mpc}}^{-1} \Psi_{mpc} x(k) = -\underbrace{K_{mpc}}_{} x(k),$$

Therefore, the control law to be applied to the plant is

$$u(k) = \Delta u(k) + u(k-1)$$

It is worth to say that the proposed predictive MPC controller can be generalized to be applied on n-inverters. As Eq. (3) indicates, to control the circulating currents flowing through n-parallel inverters, only n-1 inverters are needed to have ZSCC control.

4. Designing comparative controller

In order to demonstrate the effectiveness of the proposed control, the performance of the proposed MPC is compared to that of PI linear controller. In the following, the design of the PI controller is presented.

(A) PI controller design

The main purpose of the PI controller is to allow tracking the reference currents. The reference voltages of each single inverter can be calculated as:

$$\begin{cases} {v_{di}}^{ref} = G_p(s)({i_{di}}^{ref} - i_{di}) - \omega L_i i_{qi} + e_d \\ {v_{qi}}^{ref} = G_p(s)({i_{qi}}^{ref} - i_{qi}) + \omega L_i i_{di} + e_d \end{cases} \tag{15}$$

and

$${v_{zi}}^{ref} = G_p(s)({i_{zi}}^{ref} - i_{zi}) \tag{16}$$

where $G_p(s)$ is the transfer function of the PI controller. The closed loop transfer function, where the inner loop is considered as a first order function, is expressed as:

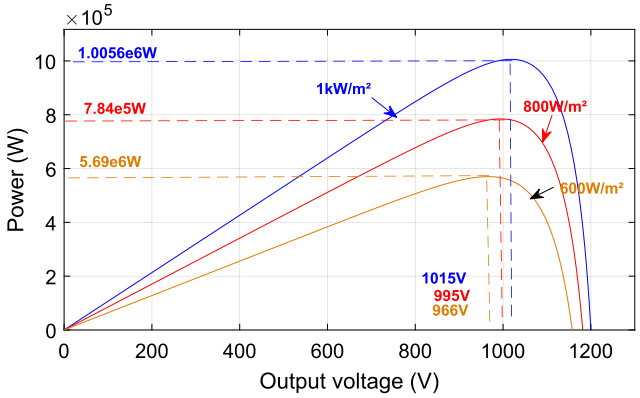

Fig. 6. Characteristics of the PV plant.

Table 1
System parameters.

Parameters	Value
Maximum Power of plant P_{max}	1,0056MW
Voltage at maximum power point of plant v_{mp}	1015V
filter resistance r	1mΩ
filter inductance L_1	300 μH
filter inductance L_2	340 μH
sampling time T_s	20 μs
fundamental frequency f	50 Hz

$$CL(s) = \frac{\frac{k_p}{L_i}s + \frac{k_i}{L_i}}{s^2 + \frac{(r+k_p)}{L_i}s + \frac{k_i}{L_i}} \tag{17}$$

Comparing this function to canonic form of a second order transfer function, we find:

$$\begin{cases} k_p = 2L_i\xi\omega_i - r \\ k_i = L_i{\omega_i}^2 \end{cases}$$

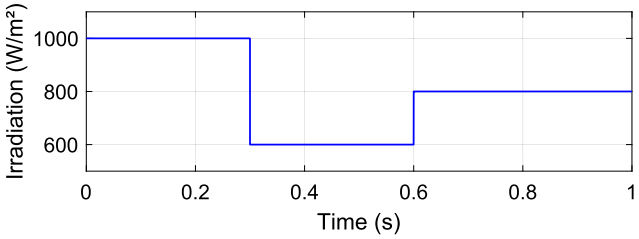

Fig. 8. Variations of irradiations.

5. Simulation results

In order to validate the proposed control strategy, a simulation of a PV system connected to the main grid with two parallel inverters is built on MATLAB/Simulink environment. The characteristics of the PV plant are shown in Fig. 6 where the generated power is about 1 MW in standard conditions (1000 W/m^2 and 25 °C). The parameters used in the simulation of the studied system are listed in Table 1.

Fig. 7 presents the Simulink block-diagram of the studied PV plant. Simpower-system Library is used to build the power part which consists of PV arrays, the paralleled inverters and connecting passive filters to the main grid. The control part consists of an MPPT algorithm and the proposed MPC controller.

Simulations are carried out during steady and transient state for the proposed MPC controller. Also, assessment and comparison of its robustness with filter parameter variations are investigated and the results of circulating current proposed are presented.

5.1. PV side power flow

Fig. 8 shows the chosen irradiation when temperature is set at 25 °C. At the beginning, the irradiation is set to 1000 W/m^2 and the maximum power injected to the grid is about 1.0056 MW as indicated in Fig. 6.

Fig. 9 shows the power extracted by the MPPT block using the well-known P&O algorithm. It is observed that in the two methods, the maximum power available is properly tracked with respect to irradiation changes. As it is shown in the results, the power ripple in case of MPC controller is less than that in case of linear controller. The percentage of the ripple in each case is respectively 0.7%, and 2.8%.

Fig. 10 illustrates the dc-link voltage; we notice that, in the two

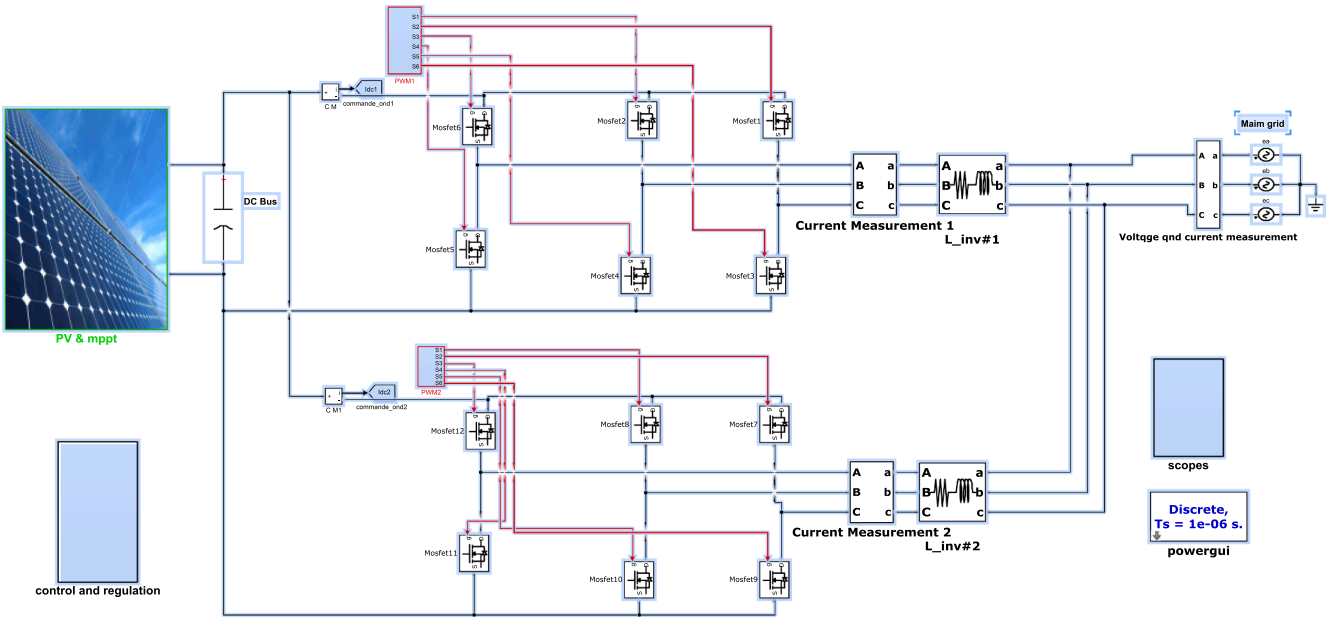

Fig. 7. Simulink block diagram of parallel inverter system.

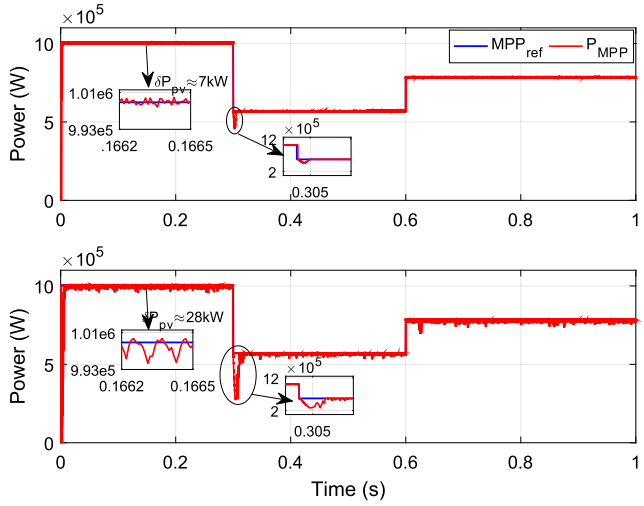

Fig. 9. Comparison of extracted power at MPP. (a) The proposed modulated MPC, (b) PI controller.

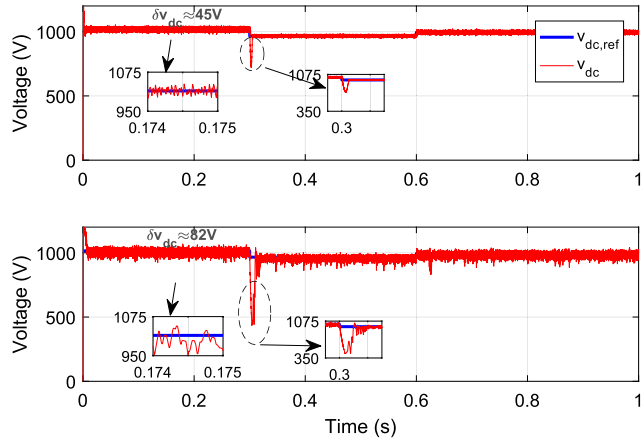

Fig. 10. Comparison of dc-link voltage. (a) The proposed MPC, (b) PI controller.

control strategies, it is kept equal to the voltage at MPP. However, the amount of the voltage ripples, in case of the proposed controller, is smaller and its value is about $\delta v_{dc} = 45V$, whereas its value in case of PI controller is $\delta v_{dc} = 82V$.

Fig. 11 shows the DC input current for the parallel inverters (i_{dc}) which is equal to the sum of (i_{dc1}) and (i_{dc2}). We notice that the input

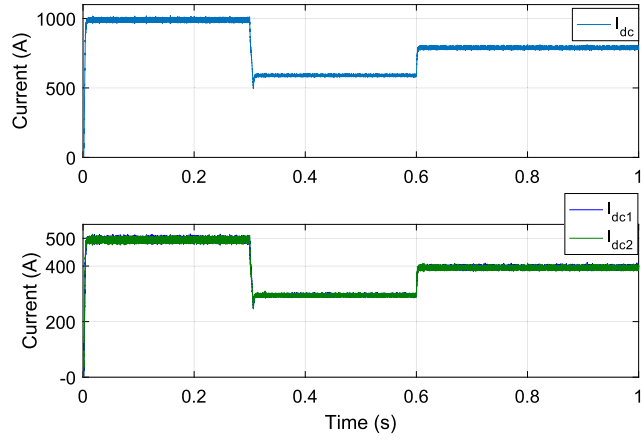

Fig. 11. The DC input current of paralleled inverters and of each inverter.

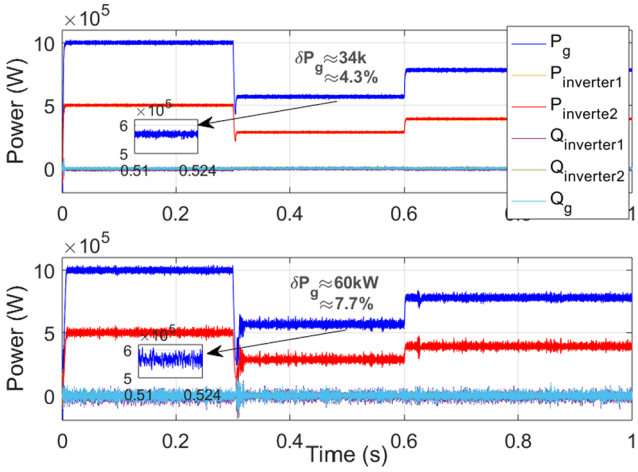

Fig. 12. Comparison of injected power into the grid: (a) the proposed modulated MPC, (b) PI controller.

power of parallel inverters is equal to the DC current times the DC link voltage.

5.2. Grid side power flow

This scenario is aimed to assess the performance of the proposed predictive controller in injecting maximum available power with respect to irradiation variations. From Fig. 12 it can be seen that the system rapidly reaches steady-state for both controllers. As it is shown, the ability of sharing power among various units is well achieved. In fact, the injected power is the sum of the power of the two inverters. One can observe that the instantaneous active and reactive power of grid side in case of the proposed controller contain smaller undesirable oscillating part which came from the power ripple that flows between DC link and RL filters. The ripple value in case of MPC is about 4.3% which is less than that in case of the PI controller which is 7.7%.

To understand well what happens in closed loop control of the PV system, either dq-current loops or circulating current loop, the next section focuses on the assessment the performance of the predictive controllers in regulating currents and suppressing circulating currents.

5.3. Current regulation performance

In this section, the performance of predictive MPC controller is investigated and compared to PI controller. The transient analysis has

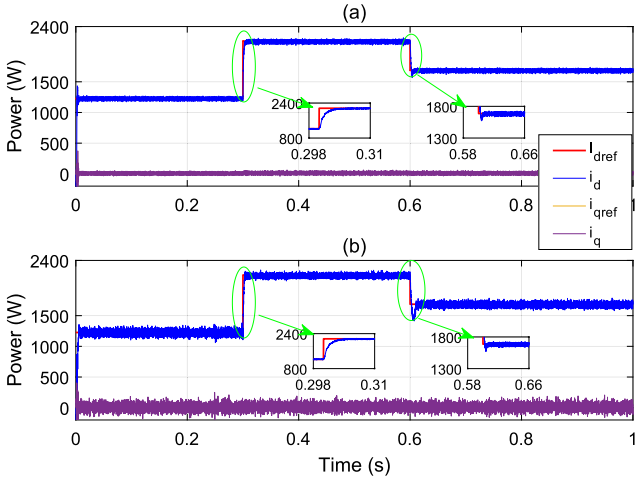

Fig. 13. Comparative simulation results of transient response in *d-q* frame: (a) the proposed modulated MPC, (b) PI controller.

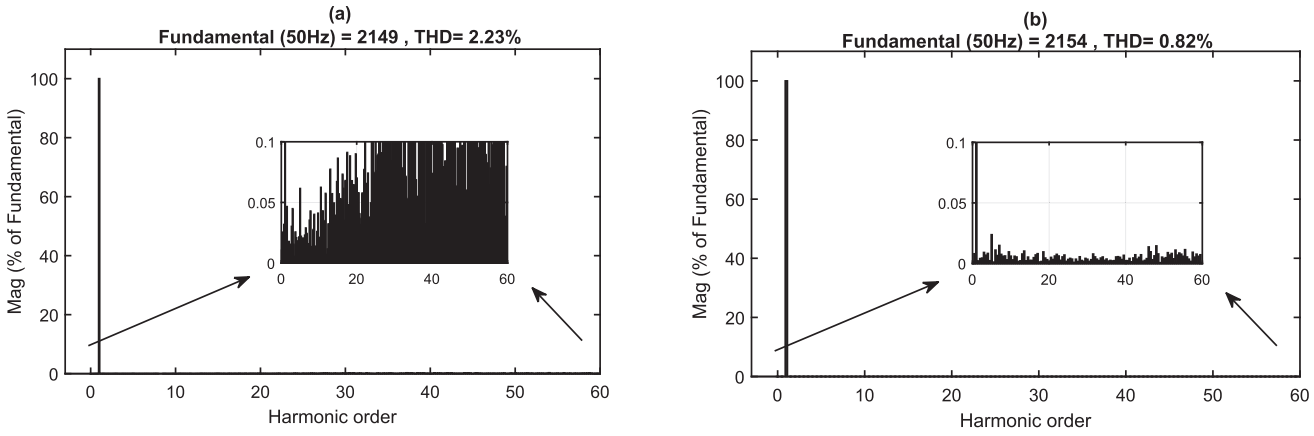

Fig. 14. The values of THD: (a) PI controller, (b) the proposed modulated MPC.

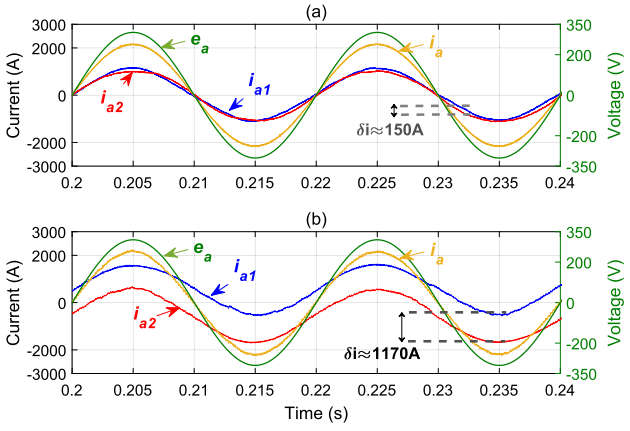

Fig. 15. The a-phase currents without zero-sequence current part; inverter line currents i_{a1}, i_{a2} and the a-phase voltage. (a) the proposed modulated MPC, (b) PI controller.

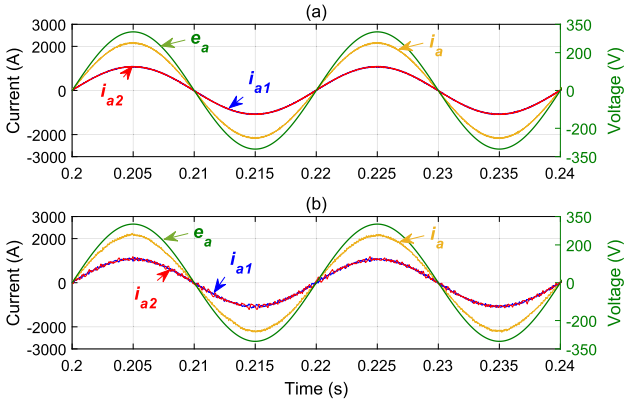

Fig. 16. The a-phase currents with zero-sequence current part; inverter line currents i_{a1}, i_{a2} and the a-phase voltage. (a) the proposed modulated MPC, (b) PI controller.

been carried out with $T_s = 20\mu s$. A step change in the irradiation is applied ($600 - 1000 - 800 W/m^2$). The obtained results are depicted in Fig. 13 where a good dynamic response of injected currents is observed. The rising time is the same in both controllers, which is about 3.7 ms. Moreover, the rejection of the disturbance using MPC is faster than that obtained by the classical controller. In terms of total harmonic distortion (THD), its value is 0.82% with MPC, whereas it is about 2.23% with PI controller (see Fig. 14). One can notice that the THD values, for

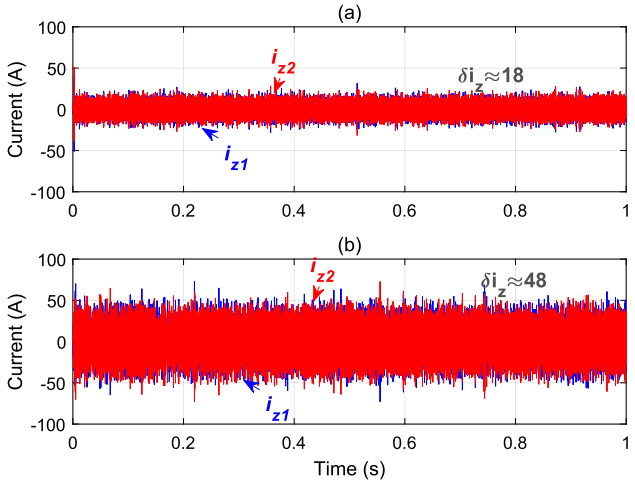

Fig. 17. Zero-sequence circulating current components i_{z1}, i_{z2} : (a) the proposed modulated MPC, (b) PI controller.

both controllers, comply with IEEE 1547 standard which must be lower than 5%.

5.4. Zero-sequence circulating current minimization

The goal of this section is to minimize the circulating current in order to increase the whole efficiency of the parallel inverters and to protect them. This is achieved by including the z-component to the cost function of controller as modelled in Section 2. Fig. 15 shows the a-phase current of each unit of the parallel inverters. It can be seen that a-phase currents are shifted from each other by ZSCC component. As depicted in the same figure, the amplitude of the ZSCC component using MPC is less even without applying ZSCC control part. Its value is $i_z = 75A$ which is about 6.85% of the injected current. Whereas its recorded value is about 53.4% when using PI controller.

As mentioned before, to handle this undesired current we need to force the z-component current to be zero and the ZSCC will track this reference. After applying zero-sequence current control, Fig. 16 reveals that a-phase currents are not shifted and ZSCC is minimized, as well as the power sharing is enhanced where the value of the a-current (i_a) is the sum of a-phase currents (i_{a1}, i_{a2}). Fig. 17 shows the minimized ZSCC component, the circulating current ripple using MPC is smaller compared to that using classical controller, and minimized better.

Fig. 18 illustrates the three-phase currents of each inverter of the studied structure after applying the ZSCC control part.

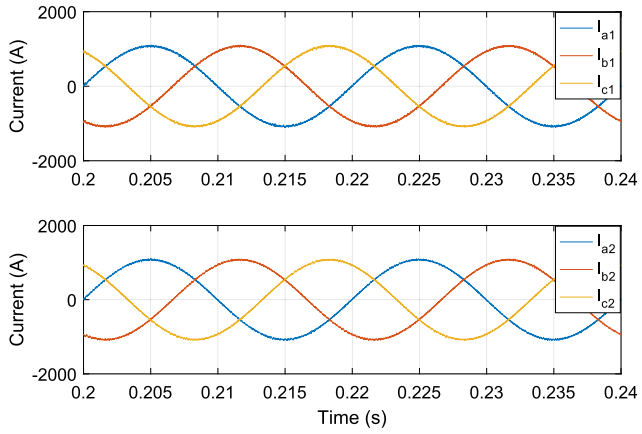

Fig. 18. The three-phase currents of each inverter of the paralleled structure.

5.5. Parameter variations & robustness analysis

This test is aimed to investigate the robustness of the proposed predictive control against filter parameter variations and compare the compensation ability for such variations. The filters are considered to change from 25%to 250% of the nominal value of the filter inductances. Fig. 19 shows the performance of the proposed predictive controller compared to PI controller in terms of harmonic contents. The Simulation confirms that both controllers are fairly good in the range of nominal value. Because MPC naturally includes uncertainties, it continues to perform properly current control for a wide range of filter parameters comparing to PI controller. Despites of 25% of the variations from the nominal value, the THD value in MPC controller is still comply with international standards. This result confirms the high performance in terms of power quality of the proposed control against filter variations.

The summary of these tests is presented in Table 2 where this plus "+" means better performance.

6. Real-time implementation in a HIL setup

A. Setup architicture

The HIL simulation prototype is built based on Opal-RT RT-LAB platform integrated with MATLAB/Simulink and dSPACE control desk. Fig. 20 describes the prepared setup used to validate the MPC control.

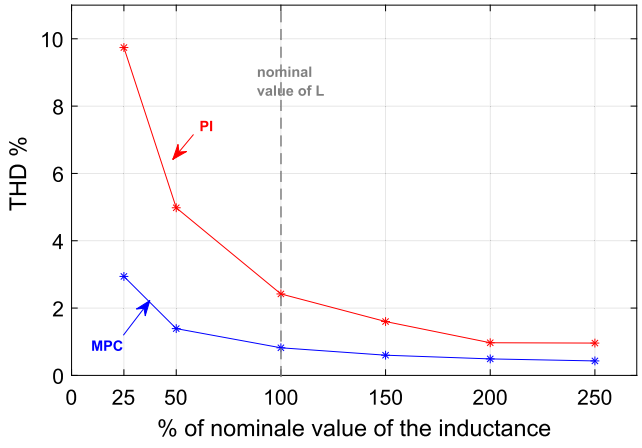

Fig. 19. Comparison of THD % (a) the proposed modulated MPC. (b) PI controller.

Table 2
Performance comparison.

Methods Criteria	Linear control	MPC control
THD	2.23%	0.82%
Rising edge time	3.7 ms	3.7 ms
Circulating current ripple	$\delta i_z \approx 48$ A	$\delta i_z \approx 18$ A
Power ripple percentage	7.7%	4.3%
Disturbance rejection	+	+ +
Robustness to model Parameters variations	+	+ +

In this setup, the physical power system is emulated in the Opal-RT OP4510 simulator and the proposed control is implemented by using a dSPACE DS 1007. The RT-LAB consists of a 3.5 GHz core, and has 128 high performance analogue/digital channels. It is controlled via windows host computer using TCP/IP connection.

B. Results

Fig. 21 shows the a-phase currents of the two parallel inverters denoted (i_{a1}, i_{a2}) and the grid current with their zoom. As it can be seen in Fig. 21(a), the presence of circulating currents results in shifting between a-phase current waveforms when the zero-sequence circulating current is uncontrolled. This undesired issue is then cancelled when activating the ZSCC control part as presented in Fig. 21(b).

The general view of the system behavior is presented in Fig. 22 where the grid voltage, the three-phase currents of the two paralleled inverters are displayed. Fig. 22(a) shows that the presence of circulating currents results in unbalanced inverter currents. Meanwhile, the activation of the ZSCC control enhances the current waveform quality and ensures equal current sharing between the two inverters Fig. 22(b).

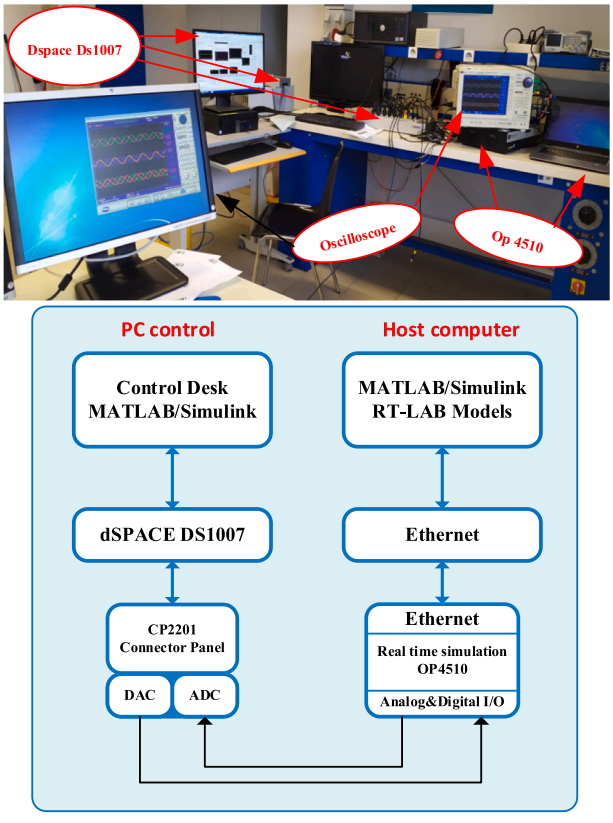

Fig. 20. HIL setup.

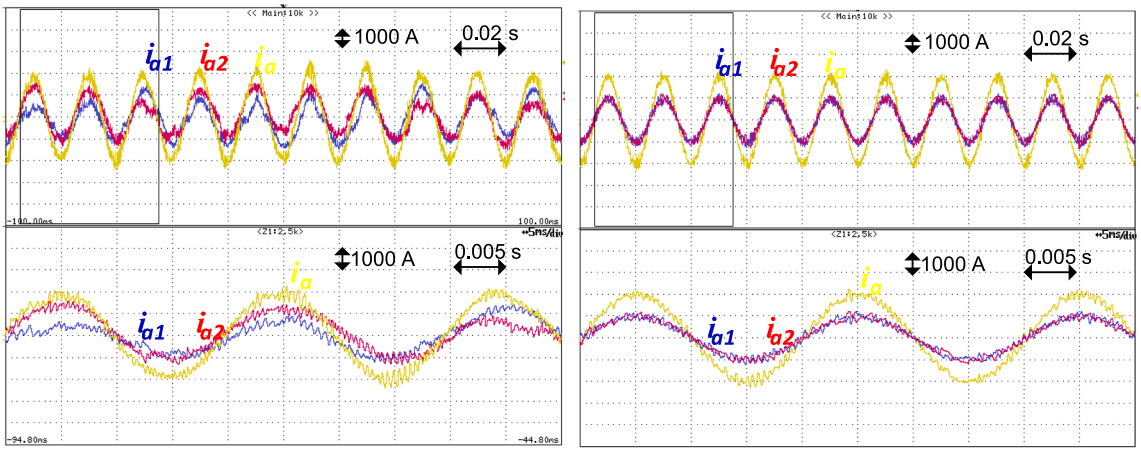

Fig. 21. HIL results of the a -phase current waveforms and their zoom: (a) without, and (b) with activating ZSCC control part.

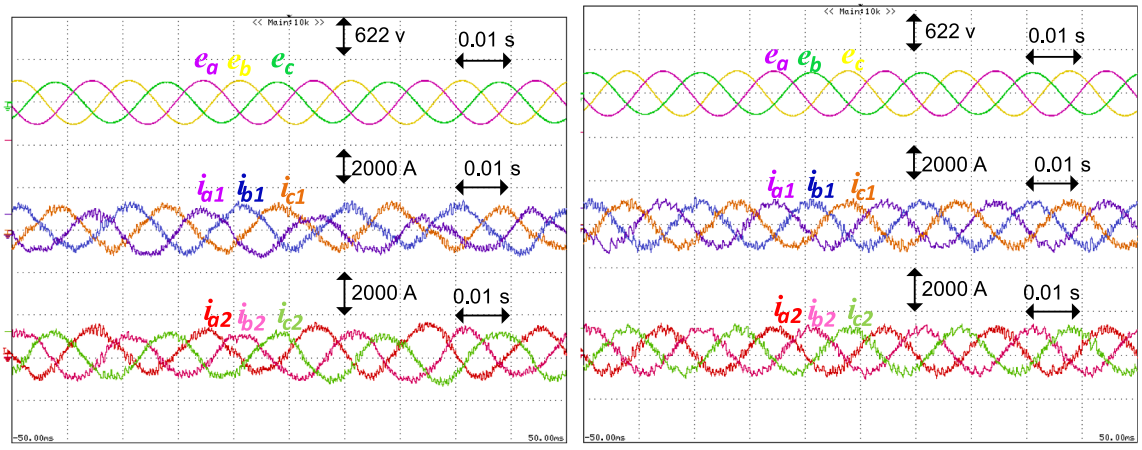

Fig. 22. HIL results of the two paralleled inverter currents and the grid voltage waveforms: (a) without, and (b) with activating ZSCC control part.

7. Conclusion

In this paper, a robust model predictive control MPC based on state-space is proposed to ensure power quality of PV plant connected to the grid with parallel inverters. The proposed control uses the optimization process in order to compute the next control which enhance the injected currents and minimize the circulating current. More, a detail designing of the proposed algorithm is presented. The proposed MPC is assessed and compared with PI control. Simulation results demonstrate that the proposed control provides good property and high performance. In case of step change, the rejection perturbation using MPC is fast. Also, the minimization of ZSCC is better where the amount of circulating current ripple is less. Moreover, MPC compensates for filter variation changes better than the linear controllers. The implementation under Hardware-In-the-Loop (HIL) setup based on Opal-RT and dSPACE rapid prototyping systems demonstrates the real-time feasibility of the proposed approach.

Declaration of Competing Interest

The authors declare that they have no known competing financial interests or personal relationships that could have appeared to influence the work reported in this paper.

Appendix A. Supplementary material

Supplementary data to this article can be found online at https://doi.org/10.1016/j.solener.2020.03.091.

References

Bella, S., Chouder, A., Djerioui, A., Houari, A., Machmoum, M., Benkhoris, M., Ghedamsi, K., 2018a. Circulating currents control for parallel grid-connected three-phase inverters. In: 2018 International Conference on Electrical Sciences and Technologies in Maghreb (CISTEM). Presented at the 2018 International Conference on Electrical Sciences and Technologies in Maghreb (CISTEM), pp. 1–5. https://doi.org/10.1109/CISTEM.2018.8613377.

Bella, S., Djcrioui, A., Houari, A., Chouder, A., Machmoum, M., Benkhoris, M., Ghedamsi, K., 2018b. Model-free controller for suppressing circulating currents in parallel-connected inverters. In: 2018 IEEE Industry Applications Society Annual Meeting (IAS). Presented at the 2018 IEEE Industry Applications Society Annual Meeting (IAS), pp. 1–6. https://doi.org/10.1109/IAS.2018.8544482.

Boukezata, B., Gaubert, J.-P., Chaoui, A., Hachemi, M., 2016. Predictive current control in multifunctional grid connected inverter interfaced by PV system. Sol. Energy 139, 130–141. https://doi.org/10.1016/j.solener.2016.09.029.

Chai, S., Wang, L., Rogers, E., 2013. Model predictive control of a permanent magnet synchronous motor with experimental validation. In: Control Engineering Practice, Advanced Software Engineering in Industrial Automation INCOM'09) 21, pp. 1584–1593. https://doi.org/10.1016/j.conengprac.2013.07.008.

Chen, T., 2009. Dual-modulator compensation technique for parallel inverters using space-vector modulation. IEEE Trans. Ind. Electron. 56, 3004–3012. https://doi.org/10.1109/TIE.2009.2022515.

Golzari, S., Rashidi, F., Farahani, H.F., 2019. A Lyapunov function based model predictive control for three phase grid connected photovoltaic converters. Sol. Energy 181, 222–233. https://doi.org/10.1016/j.solener.2019.02.005.

IEA PVPS report, 2018. Trends in photovoltaic application. http://www.iea-pvps.org/fileadmin/dam/public/report/statistics/2018_iea-pvps_report_2018.pdf.

Agency, Solar PV Tracking Clean Energy Progress, 2018, https://www.iea.org/tracking/tcep2018/power/renewables/solar/.

Jiang, W., Ma, W., Wang, J., Wang, W., Zhang, X., Wang, L., 2018. Suppression of zero sequence circulating current for parallel three-phase grid-connected converters using hybrid modulation strategy. IEEE Trans. Ind. Electron. 65, 3017–3026. https://doi.org/10.1109/TIE.2017.2750625.

Ji, Jun-Keun, Sul, Seung-Ki, 1999. Operation analysis and new current control of parallel connected dual converter system without interphase reactors. In: IECON'99.

Conference Proceedings. 25th Annual Conference of the IEEE Industrial Electronics Society (Cat. No.99CH37029). Presented at the IECON'99. Conference Proceedings. 25th Annual Conference of the IEEE Industrial Electronics Society (Cat. No. 99CH37029), vol. 1, pp. 235–240. https://doi.org/10.1109/IECON.1999.822202.

Kazmierkowski, M.P., 2012. Predictive control of power converters and electrical drives [book news]. IEEE Ind. Electron. Mag. 6, 67–68. https://doi.org/10.1109/MIE.2012.2221371.

Lim, C., Levi, E., Jones, M., Rahim, N.A., Hew, W., 2014. A comparative study of synchronous current control schemes based on FCS-MPC and PI-PWM for a two-motor three-phase drive. IEEE Trans. Ind. Electron. 61, 3867–3878. https://doi.org/10.1109/TIE.2013.2286573.

Marija Maisch, 2018. Bungala Solar Farm goes fully online as Australia's biggest solar project to date. pv magazine Australia. https://www.pv-magazine-australia.com/2018/11/05/bungala-solar-farm-goes-fully-online-as-australias-biggest-solar-project-to-date/.

Ogasawara, S., Takagaki, J., Akagi, H., Nabae, A., 1992. A novel control scheme of a parallel current-controlled PWM inverter. IEEE Trans. Ind. Appl. 28, 1023–1030. https://doi.org/10.1109/28.158825.

Ouai, A., Mokrani, L., Machmoum, M., Houari, A., 2018. Control and energy management of a large scale grid-connected PV system for power quality improvement. Sol. Energy 171, 893–906. https://doi.org/10.1016/j.solener.2018.06.106.

Prasad, J.S.S., Ghosh, R., Narayanan, G., 2015. Common-mode injection PWM for parallel converters. IEEE Trans. Ind. Electron. 62, 789–794. https://doi.org/10.1109/TIE.2014.2347914.

PVS800-Central inverters (ABB Solar inverters). https://new.abb.com/power-converters-inverters/main/solar/central/pvs800.

Quan, Z., Li, Y.W., 2017. A three-level space vector modulation scheme for paralleled converters to reduce circulating current and common-mode voltage. IEEE Trans. Power Electron. 32, 703–714. https://doi.org/10.1109/TPEL.2016.2529959.

SGI 500/750XTM Utility-Scale PV Inverter – Yaskawa – Solectria Solar. https://solectria.com/pv-inverters/utility-scale-inverters/sgi-500-750xtm/.

Tang, R., 2017. Large-scale photovoltaic system on green ship and its MPPT controlling. Sol. Energy 157, 614–628. https://doi.org/10.1016/j.solener.2017.08.058.

Tobar, C., Karina, A., 2018. Large Scale Photovoltaic Power Plants: Configuration, Integration and Control. Ph.D. Thesis. Universitat Politècnica de Catalunya.

Wang, J., Hu, F., Jiang, W., Wang, W., Gao, Y., 2018. Investigation of zero sequence circulating current suppression for parallel three-phase grid-connected converters without communication. IEEE Trans. Ind. Electron. 65, 7620–7629. https://doi.org/10.1109/TIE.2018.2798613.

Wang, L., 2009. Model Predictive Control System Design and Implementation Using MATLAB®, Advances in Industrial Control. Springer-Verlag, London.

Wei, B., Guerrero, J.M., Vásquez, J.C., Guo, X., 2017. A circulating-current suppression method for parallel-connected voltage-source inverters with common DC and AC buses. IEEE Trans. Ind. Appl. 53, 3758–3769. https://doi.org/10.1109/TIA.2017.2681620.

Wu, Y., Lin, J., Lin, H., 2017. Standards and guidelines for grid-connected photovoltaic generation systems: a review and comparison. IEEE Trans. Ind. Appl. 53, 3205–3216. https://doi.org/10.1109/TIA.2017.2680409.

Xing, X., Zhang, C., He, J., Chen, A., Zhang, Z., 2017. Model predictive control for parallel three-level T-type grid-connected inverters in renewable power generations. IET Renew. Power Gener. 11, 1353–1363. https://doi.org/10.1049/iet-rpg.2016.0361.

Xu, D., Wang, G., Yan, W., Yan, X., 2019. A novel adaptive command-filtered backstepping sliding mode control for PV grid-connected system with energy storage. Sol. Energy 178, 222–230. https://doi.org/10.1016/j.solener.2018.12.033.

Xueguang, Z., Jiaming, C., Yan, M., Yijie, W., Dianguo, X., 2014. Bandwidth expansion method for circulating current control in parallel three-phase PWM converter connection system. IEEE Trans. Power Electron. 29, 6847–6856. https://doi.org/10.1109/TPEL.2014.2311046.

Yaramasu, V., Rivera, M., Wu, B., Rodriguez, J., 2013. Model predictive current control of two-level four-leg inverters—Part I: Concept, algorithm, and simulation analysis. IEEE Trans. Power Electron. 28, 3459–3468. https://doi.org/10.1109/TPEL.2012.2227509.

Zhang, P., Zhang, G., Du, H., 2018. Circulating current suppression of parallel photovoltaic grid-connected converters. IEEE Trans. Circuits Syst. II Express Briefs 65, 1214–1218. https://doi.org/10.1109/TCSII.2017.2789215.

Ye, Zhihong, Boroyevich, D., Choi, Jae-Young, Lee, F.C., 2002. Control of circulating current in two parallel three-phase boost rectifiers. IEEE Trans. Power Electron. 17, 609–615. https://doi.org/10.1109/TPEL.2002.802170.

Zorig, A., Barkat, S., Belkheiri, M., Rabhi, A., Blaabjerg, F., 2017. Novel differential current control strategy based on a modified three-level SVPWM for two parallel-connected inverters. IEEE J. Emerg. Select. Top. Power Electron. 5, 1807–1818. https://doi.org/10.1109/JESTPE.2017.2714100.